

# Exact Zero-Modes of the Compact QED Dirac Operator

Bernd A. Berg,<sup>a</sup> Urs M. Heller,<sup>a</sup> Harald Markum,<sup>b</sup>  
Rainer Pullirsch,<sup>b</sup> Wolfgang Sakuler<sup>b</sup>

<sup>a</sup>*Department of Physics,  
and*

*School of Computational Science and Information Technology,  
The Florida State University, Tallahassee, FL 32306*

<sup>b</sup>*Atominstitut der österreichischen Universitäten, Technische Universität Wien,  
A-1040 Vienna, Austria*

---

## Abstract

We calculate the low-lying eigenmodes of the Neuberger overlap-Dirac operator for  $4d$  compact lattice QED in the quenched approximation. In the strong coupling phase we find exact zero-modes, quite similar as in non-Abelian lattice QCD. Subsequently we make an attempt to identify responsible topological excitations of the  $U(1)$  lattice gauge theory.

*Key words:* Topology, Abelian gauge theory

*PACS:* 11.15.Ha, 05.45.Pq, 12.38Ge

---

In recent years the spectrum of the Dirac operator in QCD-like theories has been related to random matrix theory (RMT), see [1] for a review. RMT reproduces the effective, finite-volume partition function results of Ref. [2]. What enters into the RMT description of the low-energy, finite-volume scaling behavior are universal symmetry properties of the Dirac operator and the topological charge and the value of the chiral condensate of the gauge configuration under consideration [3,4]. Via the Atiyah-Singer index theorem the topological charge is mapped on the number of fermionic zero-modes of the Dirac operator. The symmetry properties of the Dirac operator fall into three classes, corresponding to the chiral orthogonal, unitary, and symplectic ensembles [4]. This classification is intimately connected to the chiral symmetry properties of fermions. A good non-perturbative regularization of QCD should therefore retain those chiral symmetry properties. Based on the overlap formalism [5], such a lattice regularization emerged only recently with the

massless Neuberger overlap-Dirac operator [6] given by

$$D = \frac{1}{2} [1 + \gamma_5 \epsilon (H_w(m))] , \quad (1)$$

where  $\gamma_5 H_w(-m)$  is the usual Wilson-Dirac operator on the lattice and  $\epsilon$  the sign function. The mass  $m$  has to be chosen to be positive and well above the critical mass for Wilson fermions but below the mass where the doublers become light on the lattice.

Previously the low-lying spectrum of the operator (1) was calculated for various QCD ensembles [7] and agreement with RMT predictions was observed. In this paper we expand such calculations to compact, quenched lattice QED with the U(1) lattice gauge theory Wilson action

$$S\{U_l\} = \beta \sum_p (1 - \cos \theta_p) . \quad (2)$$

Here  $\beta = 1/g^2$ ,  $U_l = U_{x,\mu} = \exp(i\theta_{x,\mu})$ , with  $\theta_{x,\mu} \in (-\pi, +\pi]$  and  $\theta_p = \theta_{x,\mu\nu} = \theta_{x,\mu} + \theta_{x+\hat{\mu},\nu} - \theta_{x+\hat{\nu},\mu} - \theta_{x,\nu}$  for  $\nu \neq \mu$ . For  $\beta < \beta_c \approx 1.01$ , this theory is in the confinement phase, exhibiting a mass gap and monopole excitations [8]. This phase exhibits chiral symmetry breaking and the chiral condensate is, according to the Banks-Casher relation [9], determined by the small eigenvalues of the Dirac operator. Properties of the chiral phase have been studied numerically in Refs. [10–12]. In the strong-coupling limit  $\beta \rightarrow 0$ , chiral symmetry breaking follows rigorously from infrared bounds [13] and it has also been calculated explicitly [14]. For  $\beta > \beta_c$ , the theory is in the chirally symmetric Coulomb phase with a massless photon [15]. There are many interesting questions concerning the order of the transition between the two phases and the possibility of a non-trivial continuum limit for  $\beta \rightarrow \beta_c^-$  [16].

Using the staggered Dirac operator, RMT predictions for U(1) lattice gauge theory were previously investigated. In both, the strong coupling as well as the Coulomb phase, the nearest neighbor spacing distribution of the complete eigenvalue spectrum was found to be in agreement with the Wigner surmise of the unitary RMT ensemble [17], indicating quantum chaos. In the strong coupling phase, below the Thouless energy, the small eigenvalues were observed to contribute to the chiral condensate similarly as for the SU(2) and SU(3) gauge groups [18], in agreement with the chiral unitary RMT ensemble.

For non-Abelian gauge theories the topological charge is determined by the instantons [19] of the gauge configuration. The topological structure of the Abelian U(1) gauge theory is different. Therefore, our first question is whether the overlap-Dirac operator will exhibit exact zero-modes at all. To answer it, we have analyzed configurations on  $L^4$  lattices at  $\beta = 0.9$  in the confined phase

and at  $\beta = 1.1$  in the Coulomb phase. With an overrelaxation/heatbath algorithm we generated 500 configurations per lattice of linear size  $L = 4, 6$  and  $8$ . After thermalization, the configurations were separated by 100 sweeps, with each sweep consisting of 3 overrelaxation updates of each link, followed by one heatbath update. On each configuration the lowest 12 eigenvalues of the overlap-Dirac operator (1) were calculated using the the Ritz functional algorithm [20] with the optimal rational approximation of Ref. [21] to  $\epsilon(H_w(m))$  and  $m$  set to 2.3.

In the confined phase exact zero-modes of the operator (1) where indeed found and are compiled in Table 1. There  $n_0^{(\nu)}$  denotes the number of configurations on which we found a zero-mode of degeneracy  $\nu$ ;  $n_0^{(0)}$  is the number of configurations with no zero-mode. The total number of zero-modes in all produced configurations (of a given lattice size) is

$$n_0^{\text{tot}} = \sum_{\nu=1}^{\infty} \nu n_0^{(\nu)} . \quad (3)$$

The highest degeneracy observed was  $\nu = 3$ . No zero-modes were found in the Coulomb phase.

$L$	$n_0^{(0)}$	$n_0^{(1)}$	$n_0^{(2)}$	$n_0^{(3)}$	$n_0^{\text{tot}}$	$10^4 \langle \nu^2 \rangle / L^4$
4	382	118	0	0	118	9.22
6	284	199	17	0	233	4.15
8	209	229	59	3	356	2.40
$Q$	0.39	0.71	0.69			

Table 1

Exact zero-modes found in 500 configurations per lattice size  $L$ . The column  $n_0^{(\nu)}$ ,  $\nu = 0, \dots, 3$ , gives the number of configurations with  $\nu$  zero-modes,  $n_0^{\text{tot}}$  is the total number of zero-modes and the last column presents the zero-mode susceptibility. The last row gives the  $Q$  values of the two-sided Kolmogorov test [24] and shows consistency of the RMT distributions (5) with our data.

For each topological sector  $\nu$ , chiral RMT predicts the distribution of the lowest non-zero eigenvalue  $\lambda_{\min}$  in terms of the rescaled variable

$$z = \Sigma V \lambda_{\min} , \quad (4)$$

where  $V$  is the volume of the system and  $\Sigma$  the infinite volume value of the chiral condensate  $\langle \bar{\psi}\psi \rangle$  determined up to an overall wave function renormalization. For the U(1) gauge group the unitary ensemble applies and the RMT

predictions for the  $\nu = 0, 1, 2$  probability densities  $\rho_{\min}^{(\nu)}(z)$  are [22,23]

$$\rho_{\min}^{(\nu)}(z) = \frac{z}{2} \begin{cases} e^{-z^2/4} & \text{for } \nu = 0, \\ I_2(z) e^{-z^2/4} & \text{for } \nu = 1, \\ [I_2(z)^2 - I_1(z)I_3(z)] e^{-z^2/4} & \text{for } \nu = 2. \end{cases} \quad (5)$$

The chiral condensate is related to the expectation value of the smallest eigenvalue. For degeneracy  $\nu$  we have

$$\Sigma = \Sigma^{(\nu)} = \frac{\langle z^{(\nu)} \rangle}{V \langle \lambda_{\min}^{(\nu)} \rangle}, \quad (6)$$

where the result is supposed to be independent of  $\nu$  and

$$\langle z^{(\nu)} \rangle = \int_0^{\infty} dz z \rho_{\min}^{(\nu)}(z). \quad (7)$$

Using analytical and numerical integration the expectation values  $\langle z^{(\nu)} \rangle$  are easily calculated. One finds

$$\langle z^{(0)} \rangle = 1.772453851, \quad \langle z^{(1)} \rangle = 3.107798700 \quad (8)$$

$$\text{and } \langle z^{(2)} \rangle = 4.344018125. \quad (9)$$

Using these numbers, the values  $\Sigma^{(\nu)}$  follow from Eq. (6) and Table 2 collects, for the various lattice sizes and  $\nu$ 's, the results which we obtain from our data. Within our limited statistical accuracy, and allowing for some finite-size effects, the different  $\Sigma^{(\nu)}$  values are consistent with one another.

$L$	$\Sigma^{(0)}$	$\Sigma^{(1)}$	$\Sigma^{(2)}$	$\Sigma$
4	0.1264 (36)	0.1379 (47)	—	0.1291 (30)
6	0.1342 (43)	0.1322 (34)	0.1179 (66)	0.1328 (28)
8	0.1131 (42)	0.1244 (29)	0.1322 (53)	0.1206 (23)

Table 2

Estimates of the chiral condensate  $\Sigma^{(\nu)}$ , where the subscript  $\nu$  denotes the topological sector in which the estimate is obtained. The last column gives the weighted average over all topological sectors.

Next, we compare the analytical distributions  $\rho_{\min}^{(\nu)}$  (5) with our computation. For  $\nu = 0, 1$  and 2, Fig. 1 displays the exact RMT probability densities  $\rho_{\min}^{(\nu)}$  of Eq. (5) and the corresponding histograms from our data. Using the definition (4) of the  $z$ -variable and for  $\Sigma$  the  $\Sigma^{(\nu)}$  values of Table 2, all lattice

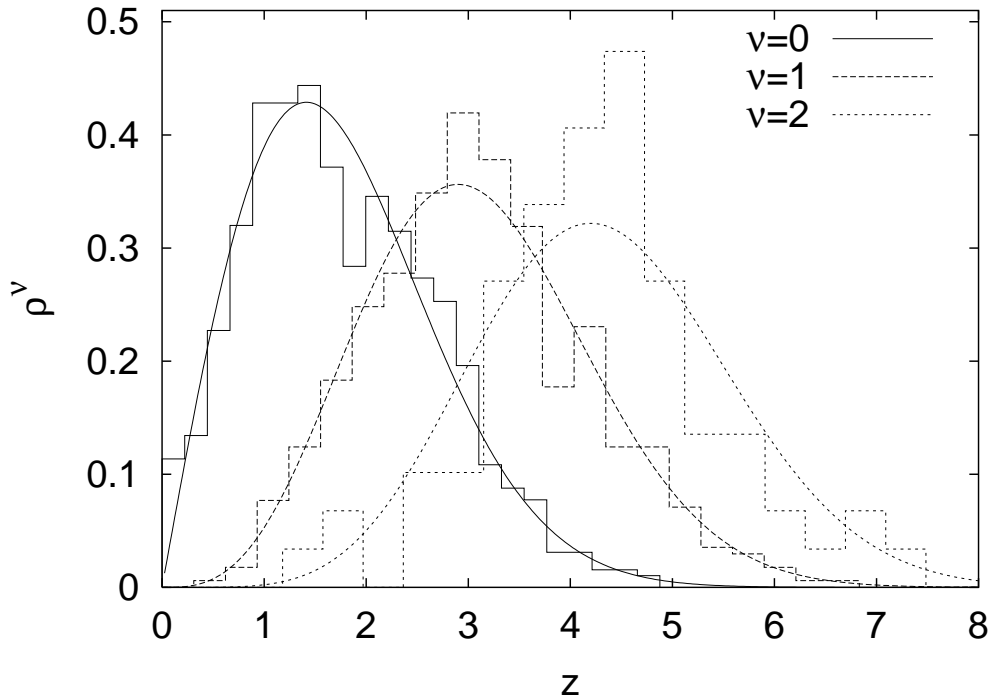


Fig. 1. The exact RMT probability densities (5) for the lowest non-zero eigenvalues are compared with histograms from our data.

sizes are combined for each  $\nu$  and the comparison is parameter free. Figure 1 shows that the histograms follow the shift of the RMT probability densities and their general shape. The high peak of the  $\nu = 2$  histogram is interpreted as a statistical fluctuation and consistent with the low statistics we have for this case. This claim is made quantitative by applying the two-sided Kolmogorov test [24] to the discrepancy between the RMT and our empirical distributions, which leads to the satisfactory  $Q$  values in the last row of Table 1. The topological structure of the U(1) gauge theory is not as extensively studied as the non-Abelian case. Nevertheless, with torons [25], monopole solutions [8] and Dirac sheets [26] a number of topological objects are known for the U(1) gauge theory and their possible relationship to the zero-modes of the overlap-Dirac operator is discussed in the remainder of this paper.

*Torons.* For a fixed link  $(x, \hat{\mu})$  we average the angle  $\phi$  over the perpendicular  $3d$  space to obtain  $\bar{\phi}_i^\mu$ ,  $i = 0, \dots, L - 1$ . We set  $\bar{\phi}_L^\mu = \bar{\phi}_0^\mu$  (periodic boundary conditions) and the sum

$$q_{\text{tor}}^\mu = \frac{1}{2\pi} \sum_{i=1}^L \bar{\phi}_{i,i-1}^\mu, \quad (10)$$

where  $\bar{\phi}_{i,i-1}^\mu$ , being the shorter distance between  $\bar{\phi}_i^\mu$  and  $\bar{\phi}_{i-1}^\mu$  on the circle, is

an integer: the toron charge for direction  $\hat{\mu}$ . Table 3 gives the distributions of the total toron charges

$$q_{\text{tor}} = \sum_{\mu=1}^4 q_{\text{tor}}^{\mu} \quad (11)$$

for all our configurations at  $\beta = 0.9$  in the confined phase. No toron charges were found at  $\beta = 1.1$  in the Coulomb phase.

$L \setminus q$	-5	-4	-3	-2	-1	0	+1	+2	+3	+4	+5
4	0	1	7	37	111	193	117	26	8	0	0
6	0	1	12	56	110	142	107	51	21	0	0
8	0	5	32	49	88	134	113	51	22	5	1

Table 3  
Distribution of the total toron charge (11).

At  $\beta = 0.9$  we checked for correlations between toron charges  $q_{\text{tor}}^{\mu}$  and  $q_{\text{tor}}$  with the degeneracy of our exact zero-modes and found none within the limitations of our statistical errors. Table 4 includes the average number of torons versus  $\nu$  (i.e. the average of the absolute values of the charges listed in Table 3). From  $L = 4$  to 6 there is an increase with lattice size, but no statistically significant dependence on  $\nu$ .

*Monopoles and Dirac sheets.* The U(1) plaquette angles  $\theta_{x,\mu\nu}$  are decomposed into the “physical” electromagnetic flux through the plaquette  $\bar{\theta}_{x,\mu\nu}$  and a number  $m_{x,\mu\nu}$  of Dirac strings passing through the plaquette

$$\theta_{x,\mu\nu} = \bar{\theta}_{x,\mu\nu} + 2\pi m_{x,\mu\nu} \quad (12)$$

where  $\bar{\theta}_{x,\mu\nu} \in (-\pi, +\pi]$ . We shall call plaquettes with  $m_{x,\mu\nu} \neq 0$  *Dirac plaquettes*. The monopole charges in elementary  $3d$  cubes are defined as the net number of Dirac strings entering or exiting these cubes. The worldlines of these monopoles on the dual lattice are closed, either within the lattice volume or by the periodic boundary conditions. The dual integer valued plaquettes

$$m_{x,\mu\nu}^* = \frac{1}{2} \varepsilon_{\mu\nu\rho\sigma} m_{x,\rho\sigma} \quad (13)$$

form Dirac sheets bounded by the worldlines of monopole-antimonopole pairs. Due to the periodic boundary conditions they can also be closed without the presence of any monopoles or antimonopoles. In the remainder we shall refer to these as *Dirac sheets*. A Dirac sheet in the x-y plane of the  $4d$  lattice must contain at least  $L_z L_t$  Dirac plaquettes. Of course, monopole loops can form

“holes” in these Dirac sheets. So, in practice we defined the number of Dirac sheets in the x-y plane as the closest integer to  $N_{1,2}/(L_z L_t)$  where  $N_{1,2}$  is the total number of Dirac plaquettes in the x-y planes.

$L$	$\nu$	Torons	Monopoles	Dirac Sheets
4	0	0.81 (04)	198.6 (1.2)	0.099 (16)
4	1	0.81 (06)	198.9 (2.0)	0.136 (32)
6	0	1.06 (05)	1007.5 (2.9)	0.106 (19)
6	1	1.08 (07)	1007.7 (3.3)	0.101 (22)
6	2	1.18 (15)	1015 (16)	0.112 (81)
8	0	1.17 (07)	3183.9 (5.7)	0.100 (21)
8	1	1.19 (07)	3195.8 (6.2)	0.100 (20)
8	2	1.46 (14)	3197 (12)	0.119 (44)
8	3	1.33 (88)	3221 (18)	none

Table 4

Average numbers of torons, monopoles and Dirac sheets per configuration with fixed zero-mode degeneracy  $\nu$ .

In the confined phase we find a large number of monopoles whereas the typical Dirac sheet numbers are 0 and  $\pm 1$  (only on the  $8^4$  lattices we found at  $\nu = 0$  a single configuration with two Dirac sheets). The average numbers of monopoles and Dirac sheets do not correlate with the topological charge  $\nu$  (i.e. our zero-mode degeneracy) as the numbers of Table 4 show. One might observe a slight increase of the monopole number with  $\nu$  which has no statistical significance. The average number of Dirac sheets shows no lattice size dependence within the limits of our statistics. In the Coulomb phase we find few monopoles and no Dirac sheets.

All these topological configurations have in common with the zero-mode degeneracy that they are turned on at the phase transition from order (Coulomb) to disorder (confined). However, in the confined phase we found no detailed correlation between any of the topological phenomena and the zero-mode degeneracy of the overlap-Dirac operator. This might be related to the fact that the zero-mode susceptibility, depicted in the last column of table 1, decreases and may approach zero for  $L \rightarrow \infty$ .

In contrast to these statistical findings there is an interesting observation that ordered Dirac sheet configurations give rise to zero-modes of the overlap-Dirac operator, with the number of zero-modes being equal to the number of Dirac sheets [5]. One might understand this from the fact that a Dirac sheet is a  $2d$  gauge configuration that contains unit topological charge in the  $2d$  sense, kept constant in the two orthogonal directions. One might even verify this

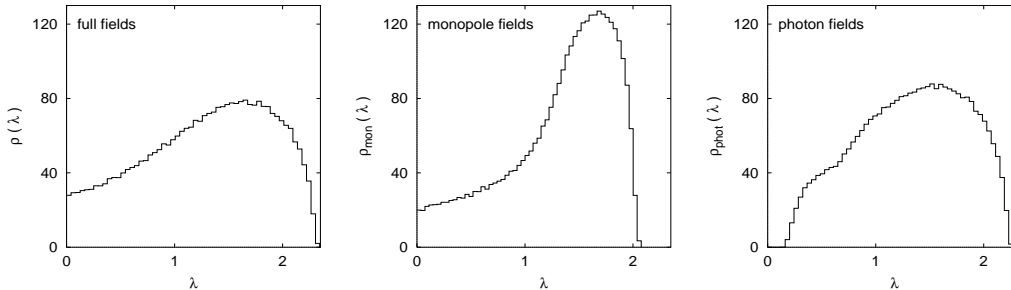


Fig. 2. Decomposition of the spectrum  $\rho(\lambda)$  (normalized to the number of eigenvalues) of the staggered Dirac operator into a monopole part  $\rho_{\text{mon}}(\lambda)$  and a photon part  $\rho_{\text{phot}}(\lambda)$ , averaged over 500 configurations on a  $4^4$  lattice.

coincidence [5] by cooling or smoothing of equilibrium gauge fields [27].

To investigate these correlations further we have, following Refs. [28,29,10], factorized our gauge configurations into monopole and photon fields in the following way

$$\theta_{x,\mu}^{\text{mon}} = -2\pi \sum_{x'} G_{x,x'} \partial'_\nu m_{x',\nu\mu} \quad (14)$$

$$\theta_{x,\mu}^{\text{phot}} = - \sum_{x'} G_{x,x'} \partial'_\nu \bar{\theta}_{x',\nu\mu} , \quad (15)$$

where  $m_{x,\mu\nu}$  and  $\bar{\theta}_{x,\mu\nu}$  are defined in Eq. (12) and

$$G_{x,x'} = \sum_{p_\mu (p \neq 0)} \frac{1}{\sum_\nu 4 \sin^2(\frac{p_\nu a}{2})} e^{ip_\mu \cdot (x_\mu - x'_\mu)} \quad (16)$$

is the lattice Coulomb propagator. One can show that  $\theta_{x,\mu} = \theta_{x,\mu}^{\text{mon}} + \theta_{x,\mu}^{\text{phot}}$  is up to a gauge transformation identical with the original  $\theta_{x,\mu}$  defined by  $U_{x,\mu} = \exp(i\theta_{x,\mu})$ .

This is a different way to probe the topological content of a gauge theory and we computed so far the total density of eigenvalues, with  $\int \rho(\lambda) d\lambda = V$ . We found that the zero-modes lie solely in the monopole part of the gauge field and are completely absent in the photonic field. Using periodic boundary conditions in space and anti-periodic boundary conditions in time [10], this was seen both for the overlap-Dirac operator and for the quasi-zero-modes of the staggered Dirac operator, see Fig. 2. At the moment we are accumulating statistics to perform a decomposition into different topological sectors and to obtain an analogous analysis as we did with the original U(1) field above. It is of further interest to study space-time correlations between different topological objects. We pose the question of the existence of local correlations between the topological charge density and the monopole density. We plan to calculate



spatial correlations with the wave functions related to fixed zero-mode number  $\nu$  and hope to understand the confining mechanism of compact QED.

*Acknowledgments:* This work was supported in part by the US Department of Energy under contract DE-FG02-97ER41022 and by the Fonds zur Förderung der wissenschaftlichen Forschung under project P14435-TPH.

## References

- [1] J.J.M. Verbaarschot, T. Wettig, *Annu. Rev. Nucl. Part. Sci.* 50 (2000) 343.
- [2] H. Leutwyler, A. Smilga, *Phys. Rev. D* 46 (1992) 5607.
- [3] E.V. Shuryak, J.J.M. Verbaarschot, *Nucl. Phys. A* 560 (1992) 306.
- [4] J.J.M. Verbaarschot, *Phys. Rev. Lett.* 72 (1994) 2531.
- [5] R. Narayanan, H. Neuberger, *Nucl. Phys. B* 443 (1995) 305.
- [6] H. Neuberger, *Phys. Lett. B* 417 (1998) 141.
- [7] R.G. Edwards, U.M. Heller, J. Kiskis, R. Narayanan, *Phys. Rev. Lett.* 82 (1999) 4188.
- [8] A.M. Polyakov, *Phys. Lett.* 59B (1975) 82; S. Mandelstamm, *Phys. Rep.* 23 (1976) 245; G. 't Hooft, *High Energy Physics*, A. Zichichi (Ed.), Editrice Compositori, Bologna, 1976; T. Banks, R.J. Myerson, J. Kogut, *Nucl. Phys. B* 129 (1977) 493; T.A. DeGrand, T. Toussaint, *Phys. Rev. D* 22 (1980) 2478.
- [9] T. Banks, A. Casher, *Nucl. Phys. B* 169 (1980) 103.
- [10] T. Bielefeld, S. Hands, J.D. Stack, R.J. Wensley, *Phys. Lett. B* 416 (1998) 150.
- [11] J. Cox, W. Franzki, J. Jersák, C.B. Lang, T. Neuhaus, *Nucl. Phys. B* 532 (1998) 315.
- [12] A. Hoferichter, V.K. Mitrjushkin, M. Müller-Preussker, H. Stüben, *Phys. Rev. D* 58 (1998) 114505.
- [13] M. Salmhofer, E. Seiler, *Commun. Math. Phys.* 139 (1991) 395.
- [14] H. Gausterer, C.B. Lang, *Phys. Lett. B* 263 (1991) 476.
- [15] B.A. Berg, C. Panagiotakopoulos, *Phys. Rev. Lett.* 52 (1984) 94.
- [16] See, e.g., J. Jersák, C.B. Lang, T. Neuhaus, *Phys. Rev. Lett.* 77 (1996) 1933 and references therein.

- [17] B.A. Berg, H. Markum, R. Pullirsch, Phys. Rev. D 59 (1999) 097504.
- [18] B.A. Berg, H. Markum, R. Pullirsch, T. Wettig, Phys. Rev. D 63 (2000) 014504.
- [19] A.A. Belavin, A.M. Polyakov, A.S. Schwartz, Yu.S. Tyupkin, Phys. Lett. 59B (1975) 85; M.F. Atiyah, N.J. Hitchin, V.G. Drinfeld, Yu.I. Manin, Phys. Lett. 65A (1978) 185; V.G. Drinfeld, Yu.I. Manin, Commun. Math. Phys. 63 (1978) 177.
- [20] B. Bunk, K. Jansen, B. Jegerlehner, M. Lüscher, H. Simma, R. Sommer, Nucl. Phys. B (Proc. Suppl.) 42 (1995) 49; T. Kalkreuter, H. Simma, Comput. Phys. Commun. 93 (1996) 33.
- [21] R.G. Edwards, U.M. Heller, R. Narayanan, Nucl. Phys. B 540 (1999) 457; R.G. Edwards, U.M. Heller, R. Narayanan, Parallel Computing 25 (1999) 1395.
- [22] P.J. Forrester, Nucl. Phys. B 402 (1993) 709.
- [23] S.M. Nishigaki, P.H. Damgaard, T. Wettig, Phys. Rev. D 58 (1998) 087704.
- [24] See, for instance, B.L. Van der Waerden, *Mathematical Statistics*, Springer, New York, 1969; W.H. Press, B.R. Flannery, S.A. Teukolsky, W.T. Vetterling, *Numerical Recipes*, Cambridge University Press, UK, 1986.
- [25] A. Gonzalez-Arroyo, J. Jurkiewicz, C.P. Korthals-Altes, NATO Advanced Study Institute, Series B: Physics 82 (1983) 339; G. 't Hooft, Nucl. Phys. B 153 (1979) 141.
- [26] V. Grösch, K. Jansen, J. Jersák, C.B. Lang, T. Neuhaus, C. Rebbi, Phys. Lett. B 162 (1985) 171.
- [27] S. Thurner, M. Feurstein, H. Markum, W. Sakuler, Phys. Rev. D 54 (1996) 3457.
- [28] J.D. Stack, R.J. Wensley, Nucl. Phys. B 371 (1992) 597.
- [29] T. Suzuki, S. Kitahara, T. Okude, F. Shoji, K. Moroda, O. Miyamura, Nucl. Phys. B (Proc. Suppl.) 47 (1996) 374.